Ejected-Atom Energy Spectra from Electronically Excited Rare-Gas Solids

D. J. O'Shaughnessy, J. W. Boring, S. Cui, and R. E. Johnson
Department of Nuclear Engineering and Engineering Physics, University of Virginia, Charlottesville, Virginia 22901
(Received 18 March 1988)

The energy spectra of atoms ejected as a result of the electronic excitation of rare-gas solids by keV electrons and He^+ ions are presented. These spectra are found to have a well-defined structure with two distinct features indicative of nonradiative electronic relaxation processes. The higher-energy peak is due to radiative decay of vibrationally relaxed dimers that are either desorbed or weakly bound to the surface. The lower-energy peak exhibits a trend from Ar to Xe which is shown to be determined by subsurface dimer decays and is consistent with the trend in the cohesive energy.

PACS numbers: 79.20.Rf

When atoms in a rare-gas solid are excited electronically by a charged particle or a photon, a number of interesting effects are observed. Excitons are produced which diffuse through the solid. These excitons may become trapped either as atomic excitons or excited dimers, with the subsequent decays involving radiative and nonradiative transitions. Since the rare-gas solids form a particularly simple class of insulators, it is desirable to be able to follow the sequence of these events in as much detail as possible. The extensive studies of the luminescence spectra from these large-band-gap, van der Waals solids have been important for describing the effect of the solid state on the interactions between individual atoms.[1,2] An important missing ingredient has been a knowledge of nonradiative relaxation processes. The observation of efficient electronically induced sputtering (desorption) of these materials[3,4] has led to studies of this aspect of the electron-hole recombination and decay sequence, as recently summarized by Reimann, Brown, and Johnson.[5] Correlations between the sputtering yield and the luminescence yield have been made for solid Ar stimulated by light fast ions,[3,5] low-energy electrons,[4] and photons.[6,7] These studies, although useful and striking, do not clearly quantify the nonradiative processes. Here we present measured kinetic energy spectra of neutral atoms ejected during electronic excitation of solid Ar, Kr, and Xe that complement the photon spectra, as well as relevant classical dynamical simulations of the sputtering process. The results clearly show that energetic, nonradiative aspects of the decay can lead to atom ejection into the vacuum. Such events are caused by localized repulsive states in the same decay sequence that results in the luminescence spectra of these materials.

We bombard low-temperature (15 K) Ar, Kr, and Xe samples (~ 1 μm thick, $< 10-$ppm impurity) in a high vacuum ($< 10^{-9}$ Torr) with 2.5-keV electrons and 33-keV He^+ ions. Although these particles can directly excite phonons, they deposit most of their energy electronically, primarily as electron-hole pairs. Absolute sputtering yields are obtained for incident He^+ ions by measuring the film thickness change for a known incident ion fluence.[8] These total-yield values are much larger than what is expected from collision-induced ejection, a fact that is consistent with measurements using light, fast ions,[3,5,9,10] or electrons.[4,11] The yield for 33-keV He^+ ions on Ar is close in value to the yields measured by

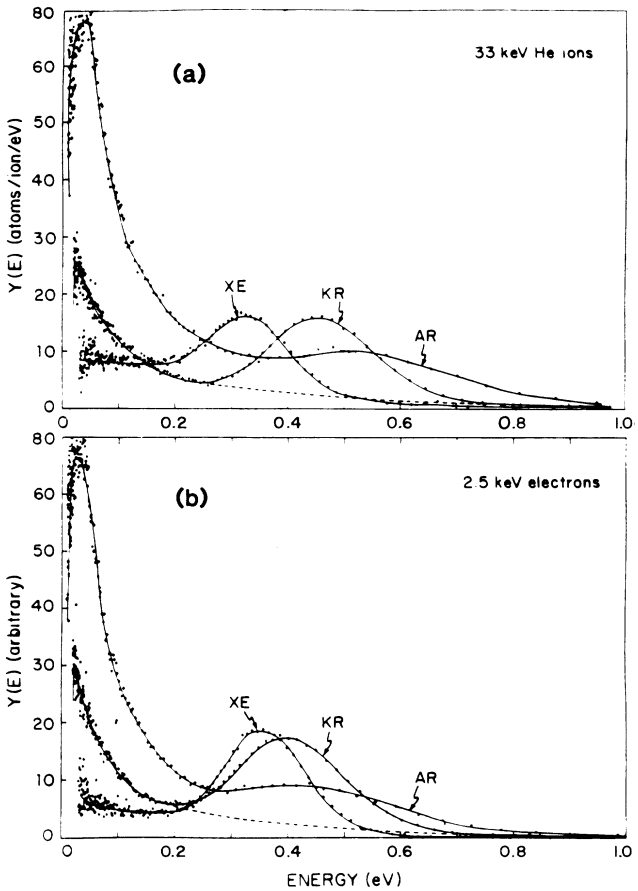

FIG. 1. Yield per unit energy vs ejected-atom energy for incident 33-keV He^+ ions on Ar, Kr, and Xe. Points are data, solid lines are drawn to guide the eye, and the dashed line indicates the extrapolation of the low-energy feature for Kr. Normalized to total yield for normal incidence (16.3, 9.9, 5.8 atoms/ion for Ar, Kr, Xe, respectively). (b) As in (a) for incident keV electrons.

TABLE I. Comparison of kinetic energy spectra and luminescence.

			Kinetic energy spectra, high-energy peak[b]			M-band luminescence[c]			
Solid	Particle[a]	Y (atoms/ion)	E (eV)	FWHM (eV)	R	$E_{h\nu}$ (eV)	FWHM/2 (eV)	$E_k/2$ (eV)	$E^*_{h\nu}$ (eV)
Ar	He^+	16.3	0.54	0.28	0.16	9.72 (9.80)	0.29 (0.30)	0.53	9.8
	e^-		0.46	0.29	0.13				
Kr	He^+	9.9	0.46	0.21	0.50	8.41 (8.48)	0.21 (0.29)	0.36	8.7
	e^-		0.40	0.22	0.60				
Xe	He^+	5.8	0.33	0.17	0.72	7.14 (7.24)	0.15 (0.25)	0.29	7.2
	e^-		0.36	0.16	1.1				

[a] He^+ at 33 keV, e^- at 2.5 keV; absolute yields Y are for He^+.

[b] E (FWHM) is position of maximum (width) after separation of low-energy contributions (see text). R is ratio of high-energy to low-energy contributions.

[c] $E_{h\nu}$ is the photon energy and FWHM/2 is the half-width of the measured M-band luminescence (Refs. 1 and 2) (second continuum in parentheses). $E^*_{h\nu}$ is the photon energy and $E_k/2$ is the repulsion energy per atom predicted by the gas-phase interatomic potentials (Refs. 13–18).

Reimann, Brown, and Johnson[5] for MeV H^+ ions at approximately equal values of the electronic stopping power. These results indicate the electronic nature of the sputtering mechanism. Sputtered-particle time-of-flight curves are obtained by use of the single-pulsed-beam technique in which neutral particles ejected perpendicular to the target surface are detected by a quadrupole mass spectrometer. The background subtraction and the conversion of the time-of-flight data to energy spectra are carried out according to the method described in Ref. 8.

The data in Fig. 1 show two distinct features. There is a peak at high energies in each case and a second feature at lower energies. In going from Ar to Xe two trends are clearly seen. The higher-energy peak shifts downward in energy, and the lower-energy feature decreases in size. The spectra for 33-keV He^+ ions on Ar, Kr, and Xe are remarkably different from the spectra obtained for heavier ions incident on these targets,[8] because of the presence of the higher-energy feature of Fig. 1(a). A similar structure in the time-of-flight curves was reported by Pedrys and co-workers.[12] It was initially assumed for incident ions that the feature at low energies was similar to the collisionally induced spectrum that we observed for the heavier incident ions.[8] However, irradiation by 2.5-keV electrons for each solid resulted in spectra nearly identical to those for He^+, Fig. 1(b). This confirms that for He^+ the dominant ejection process at all ejection energies is electronically stimulated. By subtracting the extrapolated low-energy feature we roughly separate the two components and in Table I give the ratio in area (R) of the high-energy and the low-energy contributions to the total yield, and the position and width of the high-energy feature.

Two properties of these solids are closely related to our observations. First, the dominant luminescence feature, the M band shown in Fig. 2, is broad (energies and width given in Table I). These widths are due to nonradiative processes associated with the decay of excited dimers.[1,2,5,12] Second, the cohesive energies of these solids increase with atomic number: Ar (0.0835 eV), Kr (0.115 eV), and Xe (0.159 eV).

A model for describing the sequence of events following the production of an electron-hole pair in rare-gas solids, based on gas-phase processes, has been suggested[19,20] and expanded upon.[3–5] Following electron-hole recombination a trapped dimer is formed with high probability. This species vibrationally relaxes ($\lesssim 10^{-10}$ sec), eventually emitting the dominant M-band luminescence ($\sim 10^{-9}$–10^{-6} sec) (Fig. 2). Repulsive energy is then released as kinetic energy after the radiative transition to the ground state (Fig. 2).[5,19,20] The shape of the measured kinetic energy spectra may therefore be explained as follows. The high-energy peak can be associated with a repulsive energy impulse given to the two atoms during the dissociation of a dimer on or outside the surface. The low-energy feature may be due to less energetic processes in the electron-hole decay sequence, or to energetic repulsive events occurring below the surface, a possibility which we examine below.

Since the repulsive energy is shared equally between the two atoms of the Ar_2 after the radiative transition shown in Fig. 2, the energy and width of the repulsion energy per atom should equal half that expected based on the luminescence peak. Indeed we find that for all of the targets in this study the width of the higher-energy peak is very nearly equal to half the width of the measured M-band luminescence peak, and its position is ap-

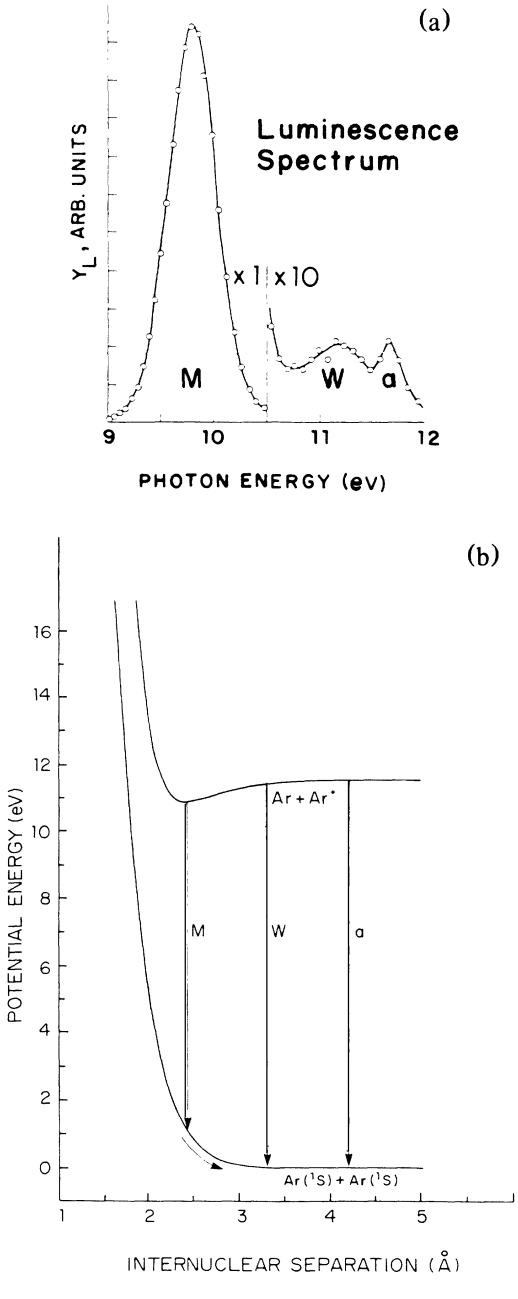

FIG. 2. (a) Low-resolution luminescence spectrum of Ar from Ref. 5. *M* and *W* are dimer decays, and *a* indicates a group of unresolved "atomic"-like decays (Refs. 1 and 2). (b) Gas-phase interaction potentials for two Ar atoms (Refs. 1, 2, 5, and 19). Transitions corresponding to luminescence spectrum indicated.

proximately half that predicted from luminescence spectra with use of gas-phase potential curves.[13-18] This agreement is evidence that the high-energy peak is primarily the result of the repulsion of ground-state atoms after radiative decay of vibrationally relaxed dimers (*M* band).

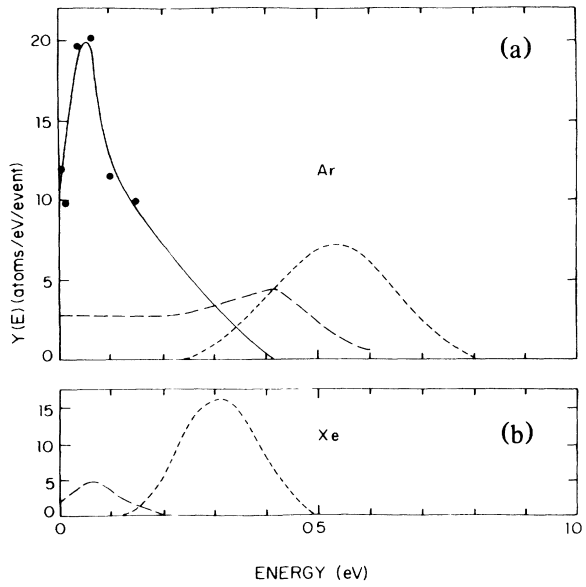

FIG. 3. Molecular-dynamics calculations of ejected-atom energy spectra: (a) solid Ar; (b) solid Xe. Short-dashed curves: energy impulse per atom following vacuum decay of a dimer (*M* band in solid phase, second continuum in gas phase). Long-dashed curves: yield from (100) face using same impulse, randomly oriented, in the first monolayer of an fcc solid. The other faces of the solid give similar results. Solid curve: yield from second and deeper layers; in Xe this is of the order of 1% of the vacuum decay peak and is not shown. All results are normalized to unit event per layer. The curves correspond to averages taken through a histogram. The points on the Ar curve give the histogram values and provide an indication of the uncertainty in the curves created by the averaging.

We also examine the effect of the material on the energy of the ejected atoms using a classical dynamics simulation.[21] In these simulations, a kinetic energy impulse equal to the ground-state repulsion energy of rare-gas atoms following the radiative decay of a dimer was given to atoms in the surface layer and at various depths below the surface with random orientations.[21,22] As the subsequent interactions proceed, the energy of particles ejected from the (100) surface of the fcc crystal is monitored. The result is an ejected-particle energy spectrum as a function of the depth at which the initial *M*-band impulse occurs.[21,22] By using a distribution of impulses determined from the potential curves and the *M*-band widths, and allowing the impulses to occur at various depths, contributions to the ejected-particle energy spectra are simulated. The results for Ar and Xe are displayed in Fig. 3. The short-dashed curves are the energy distributions for dimer decay in the vacuum. The long-dashed curves reveal the important effect of surface binding on ejection from the surface layer. Decay in an undistorted surface leads to predictions of ejected-particle energy spectra shifted to considerably lower energy than the gas-phase repulsive energy per atom and

lower than the energy of our experimental high-energy peak. The solid curves in Fig. 3, show the dominant effect of collisions in the solid if the initial energy release is below the surface. The suppression of ejection for subsurface energy releases is greatly increased in going from Ar to Xe so that only the surface layer contributes in the latter case. This is a trend that is clearly seen in the data of Fig. 1. The experimental curves of Fig. 1 can be very nearly duplicated by a suitable weighting of the three (or two for Xe) simulation spectra of Fig. 3. In this weighting, the higher-energy peaks in the ejected-particle energy spectra are associated with the repulsion of ground-state atoms in an environment in which there is little interaction with the other atoms (e.g., decay in the vacuum, away from the surface, or on the surface with a cavity distortion of the lattice around the dimer).

This quantitative comparison depends on the ability of the gas-phase potentials to describe the excited states in the rare-gas solids and the ability of the dimers to vibrationally relax before ejection.[4,5,23] The M-band photon energies predicted by the gas-phase potentials (Table I) are in good agreement with the measured photon energies. However, for reasonable changes in the potential, one must still allow vibrational relaxation in order to achieve the consistency observed between the width of the kinetic energy spectra and that of the M bands (Table I). This relaxation can be caused by a precursor process (e.g., electron-hole recombination[5]) or occurs in conjunction with the lattice distortion about the dimer.[4]

From this discussion one can draw the following conclusions about the ejected-particle energy spectra for Ar, Kr, and Xe targets sputtered by keV He^+ ions and electrons: The observation of clear peaks in the energies of ejected particles for all these solids demonstrates that repulsive decays of a very definite energy are the major contributor to the electronic sputtering of rare-gas solids. For all three targets the position and width of the higher-energy peak are close to the predicted repulsion energy per atom following radiative decay (M band) of vibrationally relaxed excited dimers, with use of gas-phase potential curves and no surface binding. Simulations of the sputtering process show that the lower-energy feature can be explained by the same repulsive dissociation events occurring within the solid. In particular, the simulations show the larger importance of the low-energy ejecta for Ar compared with Xe due to the lower cohesive energy of Ar, which allows a larger contribution from impulses occurring several layers beneath the surface. These studies have given information concerning the energetics of the nonradiative aspects of electronic relaxation in rare-gas solids. They have indicated that a primary mechanism for producing the observed kinetic energies is described by radiative decay of an electronically excited, vibrationally relaxed dimer having at most a very small center-of-mass energy. The relative importance of vacuum, surface, and subsurface impulses has been studied by comparing computer simulations to the measured spectra.

This work is supported by National Science Foundation Grant No. DMR-86-00469.

[1]See, for example, *Electronic Excitations in Condensed Rare Gases,* edited by N. Schwentner, E. E. Koch, and J. Jortner, Springer Tracts in Modern Physics Vol. 107 (Springer-Verlag, Berlin, 1985).

[2]See, for example, G. Zimmerer, in *Excited-State Spectroscopy In Solids,* International School of Physics "Enrico Fermi," Course XCVI, edited by U. M. Grassano and N. Terzi (Societa Italiana di Fisica, Bologna, Italy, 1987), pp. 37–110.

[3]C. T. Reimann, R. E. Johnson, and W. L. Brown, Phys. Rev. Lett. **53**, 600 (1984).

[4]F. Coletti, J. M. Debever, and G. Zimmerer, J. Phys. (Paris) Lett. **45**, L467 (1984).

[5]C. T. Reimann, W. L. Brown, and R. E. Johnson, Phys. Rev. B **37**, 1455 (1988).

[6]T. Kloiber, W. Laasch, G. Zimmerer, F. Coletti, and J. M. Debever, Europhys. Lett. (to be published).

[7]P. Feulner, T. Muller, A. Poschmann, and D. Menzel, Phys. Rev. Lett. **59**, 791 (1987).

[8]D. J. O'Shaughnessy, J. W. Boring, J. A. Phipps, and R. E. Johnson, Surf. Sci. (to be published).

[9]F. Besenbacher, J. Bottiger, O. Graversen, J. L. Hansen, and H. Sorensen, Nucl. Instrum. Methods **191**, 221 (1981).

[10]J. Schou, O. Ellegaard, H. Sorensen, and R. Pedrys, Nucl. Instrum. Methods Phys. Res. (to be published).

[11]J. Schou, Nucl. Instrum. Methods Phys. Res., Sect. B **27**, 188 (1987); J. Schou, P. Borgesen, O. Ellegaard, H. Sorensen, and C. Claussen, Phys. Rev. B **34**, 93 (1986).

[12]R. Pedrys, D. J. Oostra, and A. E. de Vries, in *Desorption Induced by Electronic Transitions: Diet II,* edited by W. Brenig and D. Menzel (Springer-Verlag, Berlin, 1985), p. 190; R. Pedrys, D. J. Oostra, A. Haring, and A. E. de Vries, to be published.

[13]R. A. Aziz and H. H. Chen, J. Chem. Phys. **67**, 5719 (1977).

[14]M. C. Castex, M. Morlais, F. Spiegelmann, and J. P. Malrieu, J. Chem. Phys. **75**, 5006 (1981).

[15]R. A. Azia, Mol. Phys. **38**, 177 (1979).

[16]F. X. Gadea, F. Spiegelmann, M. C. Castex, and M. Morlais, J. Chem. Phys. **78**, 7270 (1983).

[17]J. A. Barker, M. L. Klein, and M. V. Bobetic, IBM J. Res. Dev. **20**, 222 (1976).

[18]M. C. Castex, J. Chem. Phys. **74**, 759 (1981).

[19]R. E. Johnson and M. Inokuti, Nucl. Instrum. Methods Phys. Res. **206**, 289 (1983).

[20]C. Claussen, Ph.D. thesis, Odense University, 1982 (unpublished); P. Borgesen, J. Schou, H. Sorensen, and C. Claussen, Appl. Phys. A **29**, 57 (1982).

[21]S. Cui, R. E. Johnson, and P. Cummings, to be published.

[22]B. J. Garrison and R. E. Johnson, Surf. Sci. **148**, 388 (1984).

[23]E. Roick, R. Gaethe, P. Gurtler, T. O. Nordruff, and G. Zimmerer, J. Phys. Chem. **17**, 945 (1984).